Published in Journal of the Geological Society, London 164, 829–842, 2007
which should be used for any reference to this work

Tectonic and metamorphic evolution of the Temsamane units, External Rif (northern Morocco): implications for the evolution of the Rif and the Betic–Rif arc

F. NEGRO[1,2], P. AGARD[3], B. GOFFÉ[1] & O. SADDIQI[4]
[1]*Laboratoire de Géologie, UMR 8538 du CNRS, Ecole normale supérieure, 24 rue Lhomond, 75231 Paris Cedex 05, France*
[2]*Present address: Institut de Géologie, Université de Neuchâtel, 11 rue Emile Argand, CP158, 2009 Neuchâtel, Switzerland (e-mail: francois.negro@unine.ch)*
[3]*Laboratoire de Tectonique, UMR 7072, Université Pierre et Marie Curie, 4 place Jussieu, 75252 Paris Cedex 05, France*
[4]*Département de Géologie, Faculté des Sciences, Université Hassan II Aïn Chock, BP 5366, Maârif Casablanca, Morocco*

Abstract: Located at an intermediate position in the External Rif nappe pile, the Temsamane units (northern Morocco) are characterized by an abnormally intense metamorphism and a penetrative ductile deformation. We present new metamorphic data showing that, in spite of their external position in the Rif, part of the Temsamane units underwent medium-pressure low-temperature (MP–LT) metamorphism (at *c*. 7–9 kbar and 330–430 °C), possibly during the Oligocene. Structural data show that the exhumation of these units, during Middle to Late Miocene times, was characterized by an intense approximately east–west stretching and by top-to-the-west shear senses. We tentatively propose two possible origins for the MP–LT Temsamane units: (1) an internal origin related to the subduction and the HP–LT event recorded in the Internal Rif (Alboran Domain), or (2) an external origin, implying a second subduction system within the External Rif, parallel to and almost contemporaneous with that of the Alboran Domain. This tectonometamorphic evolution of the Temsamane units is set within the context of the External Rif evolution. At a larger scale, we show that the exhumation history of the Temsamane units, which strongly resembles that documented in the core of the internal Betics, is compatible with the westward slab retreat occurring during the Middle to Late Miocene in the Betic–Rif region.

The Rif (northern Morocco) and the Betics (southern Spain) represent the western termination of the Alpine orogenic system, which resulted from the plate convergence between Africa and Eurasia since late Mesozoic times (e.g. Dewey *et al*. 1989; Jolivet *et al*. 2003; Chalouan & Michard 2004). The arc-shaped Rif fringes the Alboran Sea and extends eastward from Morocco to the Algerian Tell (Fig. 1a). It comprises the internal, Alboran Domain units associated with subduction–collision processes and burial (e.g. Azañón & Crespo-Blanc 2000; Jolivet *et al*. 2003; Michard *et al*. 2006), and the non-metamorphic units from the External Rif nappe stack (Frizon de Lamotte 1987; Chalouan *et al*. 2001).

Within the External Rif nappe stack, however, the Temsamane units (Fig. 1a) are characterized by low-grade greenschist-facies metamorphism and a penetrative ductile deformation (Frizon de Lamotte 1985). Suter (1980) first imagined that they could have an internal origin related to the Alboran Domain, and preliminary ^{40}Ar–^{39}Ar constraints on metamorphism yielded an Oligocene age (Monié *et al*. 1984). However, the origin, the age and the tectonic evolution of these metamorphic units have remained largely unclear and precise P–T conditions are lacking.

Such metamorphism, and associated deformation, in the external Rif challenges our understanding of the geodynamic evolution of the Rif chain, and of the Betic–Rif arc within the frame of the Africa–Eurasia convergence. We present below the results of a detailed petrological study and the first P–T estimates for the Temsamane units, together with a coupled analysis of ductile and brittle deformation. We then discuss the tectonometamorphic evolution of these units and its implications for regional geodynamics.

Geological setting

Regional geology

The Rif chain is classically divided into several geological domains: the External Rif, the Flysch units and the Internal Rif, also known as the Alboran Domain (Fig. 1a; Suter 1980).

The External Rif nappe stack, made of Triassic to Neogene sedimentary cover units (Wildi 1983), is classically divided into the Prerif, Mesorif and Intrarif domains. Parts of the Mesorif and Intrarif were detached during the Miocene to form allochthonous nappes (External Rif nappes). All these units are non-metamorphic, except for some of the Temsamane units and the Ketama units (Fig. 1a), which recorded low-grade greenschist-facies metamorphism (Andrieux 1973; Frizon de Lamotte 1985). Serpentinites underlying the Ketama units (Beni Malek massif) are interpreted as relict mantle units exhumed during the Tethyan rifting (Michard *et al*. 1992). Flysch nappes (Intrarif; Fig. 1a), composed of Liassic to Oligocene sediments, were deposited on highly thinned continental or oceanic crust (Durand-Delga *et al*. 2000).

The Alboran Domain represents the Internal Zones of both the Rif and the Betics (Fig. 1a and b). It mainly consists of a stack of metamorphic nappes, including peridotite slivers, divided into the Sebtide and Ghomaride complexes and the Dorsale calcaire units. The Sebtide complex, equivalent to the Alpujárride complex in the Betics, recorded high-pressure low-temperature (HP–LT) conditions (Bouybaouène *et al*. 1995). The non-metamorphic, Dorsale units were interpreted by some as the cover of the Sebtide units (Didon *et al*. 1973).

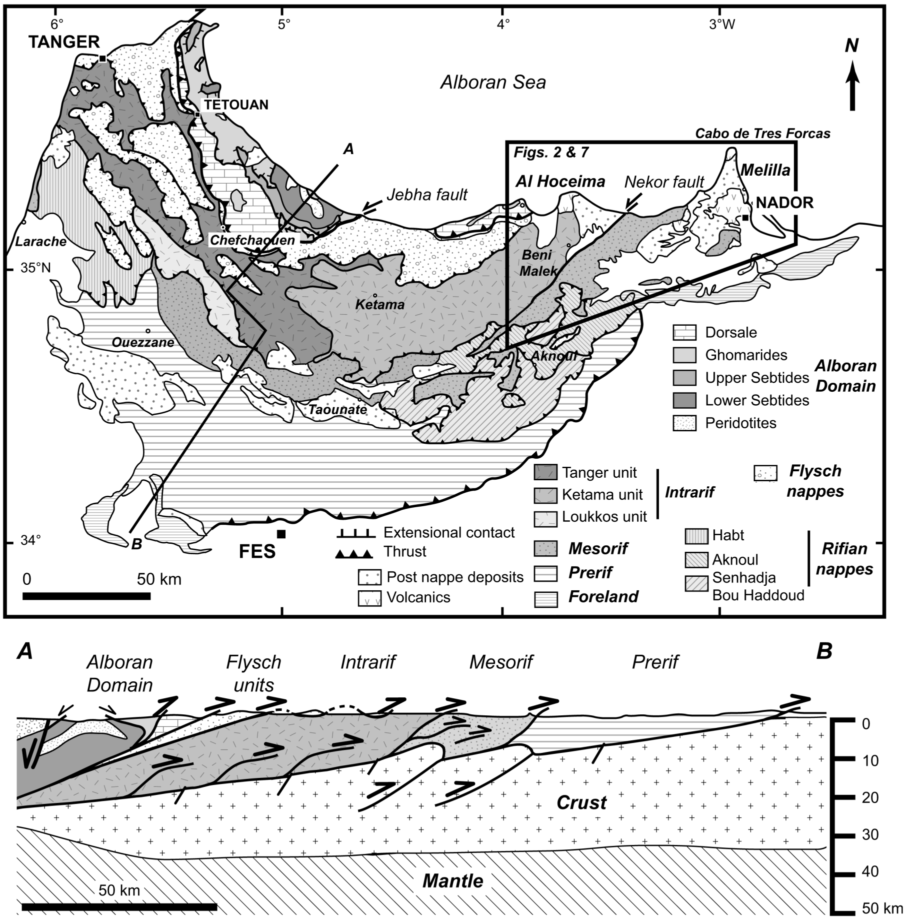

Fig. 1. (**a**) Geological and tectonic map of the Rif. Modified after Frizon de Lamotte (1987) and Chalouan *et al*. (2001) for the External Rif. (**b**) Crustal-scale cross-section of the Rif, modified after the Transmed transect (Frizon de Lamotte *et al*. 2004).

The structure and the tectonic style of the External Rif are dominated by major southward-directed thrusts that bound the various domains (Fig. 1a and b; Chalouan *et al*. 2001). The main tectonic phase in the External Rif is Middle to Late Miocene in age (Frizon de Lamotte *et al*. 2004). Two major left-lateral fault zones, Jebha and Nekor, have also been active since the Early Miocene (Late Burdigalian) and the Late Miocene (Tortonian), respectively (Leblanc 1990; Asebriy *et al*. 1993).

The External Zones in the eastern Rif

Regional geology of the eastern Rif. The Temsamane units (Mesorif) crop out in the eastern part of the Rif, between Al Hoceima and Melilla (Fig. 1a). This massif is elongated NE–SW, and is bounded to the west by the Nekor sinistral strike-slip fault, and to the south by the Rif foreland units and the External Rif nappes (Fig. 2a). The Ketama unit is composed of Triassic–Liassic to Upper Cretaceous low-grade metamorphic sediments (Frizon de Lamotte & Leikine 1985). The Aknoul nappe, of Intrarif origin, represents the cover of the Ketama unit (Frizon de Lamotte 1985) and is composed of Upper Cretaceous to Oligocene non-metamorphic sediments. The Senhadja and Bou Haddoud nappes, of Mesorifan origin, comprise probable Palaeozoic to Middle Miocene sediments (Wildi 1983). All these units are unconformably overlain by Messinian to Pliocene sediments (Fig. 2a).

Lithostratigraphy and structure of the units. The stratigraphy and structure of the Temsamane units presented here is based on the work of Frizon de Lamotte (1985) (Fig. 2a and b). The Temsamane units are composed of Mesozoic to Cenozoic sedimentary units with rare mafic intercalations (Fig. 3). The massif can be divided into seven distinct tectonic units (Fig. 2a and b), each with its own stratigraphic succession (Fig. 3). The units are bounded by north-dipping thrusts, which strike parallel to the length of the massif (Fig. 2a and b). We also assign the Tres Forcas (VIII) and Khebaba units (IX) to the Temsamane group on the basis of metamorphic characteristics. The Ras Afraou, Tres Forcas and Khebaba units were interpreted as allochthonous units belonging to the Alboran Domain (Fig. 2a; Suter 1980). However, the Ras Afraou unit was assigned to the Temsamane units by Frizon de Lamotte (1985). Furthermore, the Khebaba unit is interpreted as an allochthon on top of the Aknoul nappes (Hervouet 1981), or as part of the Senhadja–Bou Haddoud group located below the Aknoul nappe (Frizon de Lamotte 1985; Darraz & Leblanc 1989). We consider that the Khebaba unit does indeed underlie the Aknoul nappe, and will discuss its origin after presenting new petrological data.

Constraints on the tectonometamorphic evolution of the Temsamane units. Only qualitative constraints were available on the tectonometamorphic evolution of the Temsamane units, based on an XRD study by Frizon de Lamotte & Leikine (1985). The North Temsamane units were considered to have experienced only low-grade metamorphism with chlorite–muscovite–paragonite–quartz assemblages, with increasing metamorphic grade towards the north. The South Temsamane units are affected by only very low-grade, anchizonal metamorphism postdating the

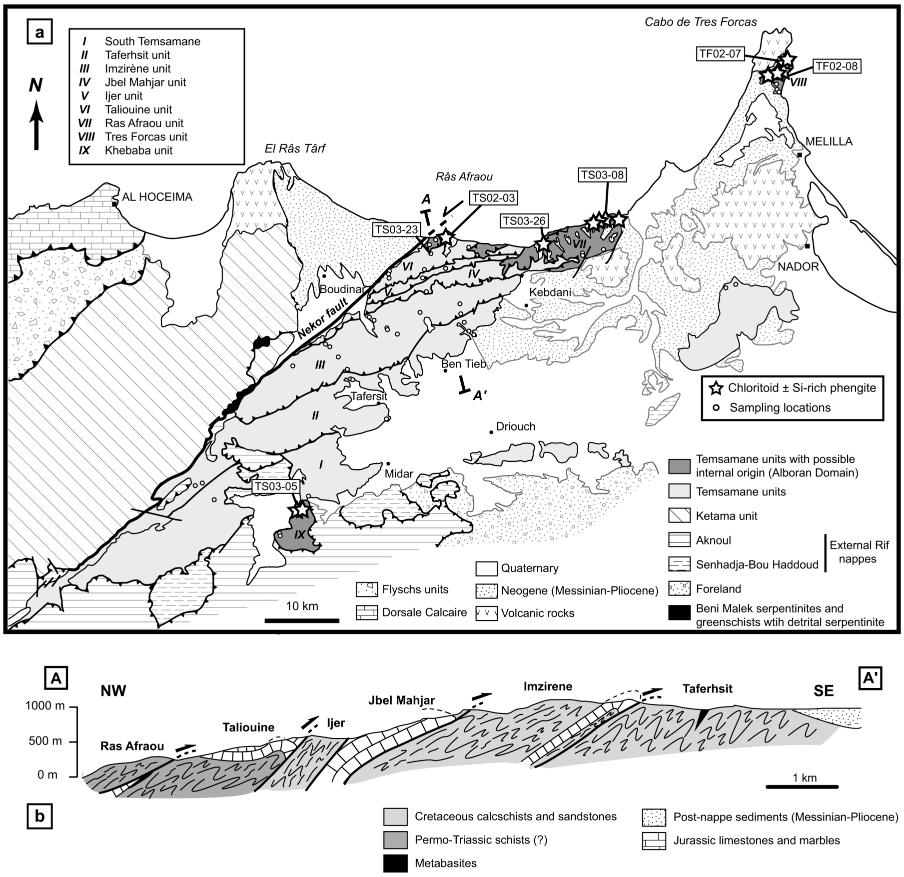

Fig. 2. (**a**) Geological map of the Temsamane units (modified after Frizon de Lamotte 1987) showing sampling locations and index mineral assemblages (for location see Fig. 1a). (**b**) Section across the North Temsamane units along the transect A–A′.

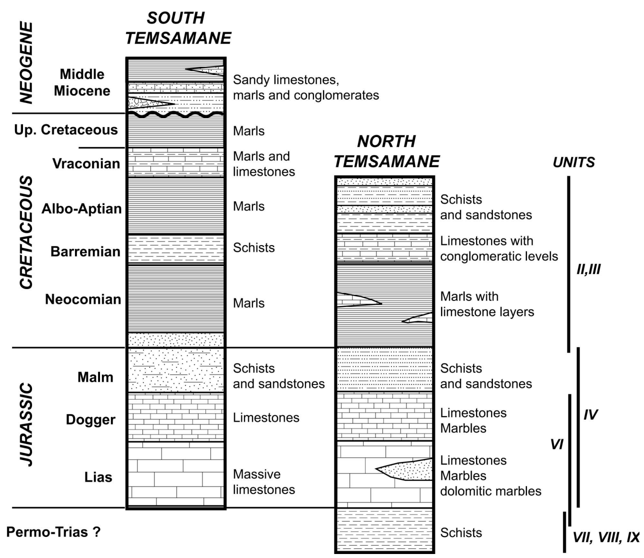

Fig. 3. Lithostratigraphic columns (not to scale) of the Temsamane units (modified after Frizon de Lamotte 1985).

Mid-Miocene (Frizon de Lamotte 1985). Few geochronological data are available to constrain the age of metamorphism and exhumation of the Temsamane units, with ages ranging between 28 and 8 Ma (Monié *et al*. 1984). Unpublished preliminary ^{40}Ar–^{39}Ar data (Negro 2005) also give ages ranging between 23 and 8 Ma.

New petrological constraints on the evolution of the Temsamane units

To quantify the metamorphism in the Temsamane units we extensively sampled all of them (Fig. 2a). Our observations are consistent with previous work, with almost non-metamorphic South Temsamane units and increasing metamorphic grade towards the north. The new index minerals reported in this study are chloritoid and high Si-content phengite. These minerals are found only in the Ras Afraou, Tres Forcas and Khebaba units, and their occurrences are reported in Figure 2a.

Mineral assemblages

Characteristic assemblages observed in the Temsamane units are reported in Table 1. In the Taferhsit, Imzirène, Ijer and Taliouine units, mineral assemblages are very similar and comprise chlorite–phengite–quartz ± albite. The small metabasite lenses found in the Taliouine unit are characterized by tremolite–epidote–albite–chlorite–sphene assemblages (Fig. 4a). The metamorphic assemblages observed in the Ras Afraou and Tres Forcas units are very similar and comprise chlorite–phengite–quartz ± chloritoid ± kaolinite ± paragonite. Albite is also present together with quartz in synfolial quartz veins or as sheared porphyroblasts in the foliation. Phengite defines the foliation and is associated with chlorite and/or kaolinite (Fig. 4b). Chloritoid marks the main foliation together with phengite or is preserved in pre-S_2 blasts and often replaced by kaolinite in the Ras Afraou and Tres Forcas units (Fig. 4c–e). In the Khebaba unit the main assemblage is composed of chloritoid–chlorite–phengite–quartz (Fig. 4f).

Table 1. *Mineral assemblages observed in the Temsamane units*

Mineral	Taferhsit Schist	Imzirene Schist	Ijer Schist	Taliouine Schist	Taliouine Metabasite	Ras Afraou Schist	Trois Fourches Schist	Khebaba Schist
Chloritoid						×	×	×
Phengite	×	×	×	×		×	×	×
Paragonite						×	×	
Chlorite	×	×	×	×	×	×	×	×
Kaolinite						×	×	
Albite	×	×			×	×	×	
Quartz	×	×	×	×		×	×	
Calcite	×	×				×	×	×
Epidote					×			
Tremolite					×			
Sphene					×			
Allanite						×		

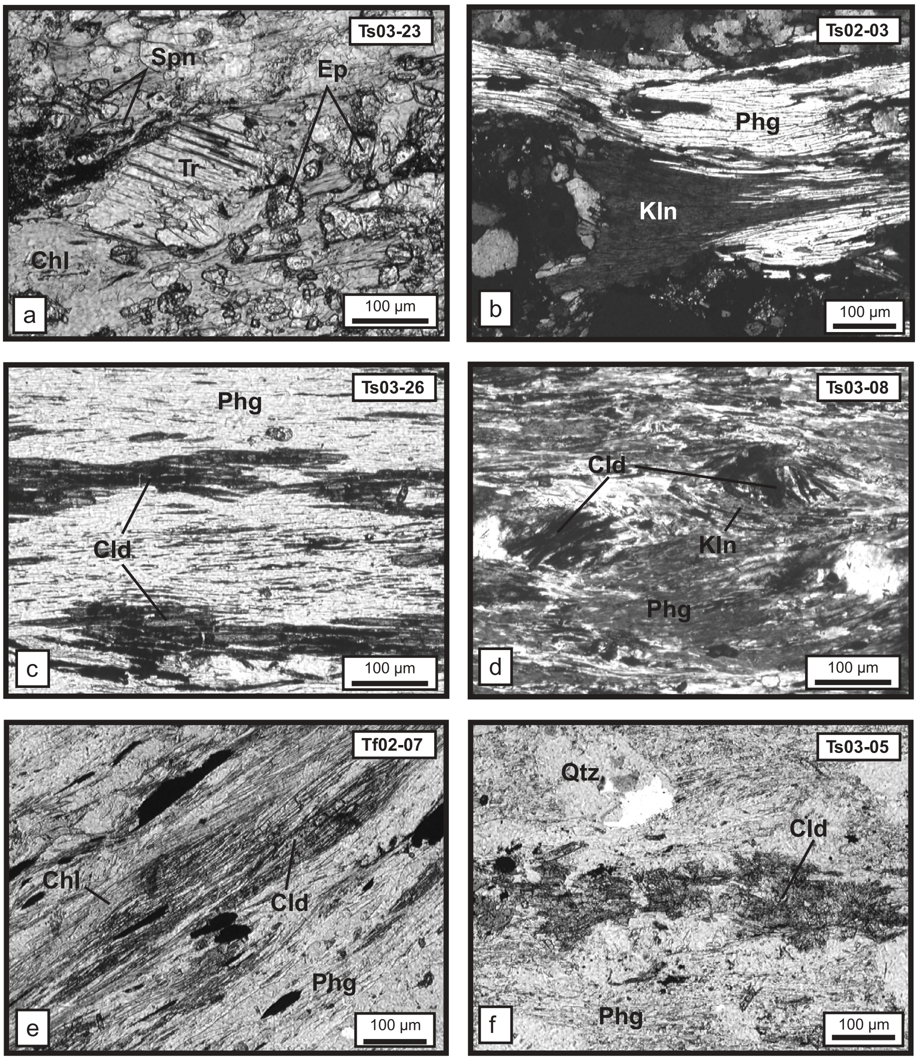

Fig. 4. Microphotographs of the metamorphic assemblages in the Temsamane units. Sample locations are shown in Figure 2a. (**a**) Epidote–chlorite–tremolite–sphene assemblage in the metabasic lenses of the Taliouine unit (plane-polarized light). (**b**) Phengite and kaolinite in the foliation of the Ras Afraou unit (crossed polars). (**c**) Chloritoid and phengite in the main foliation of the Ras Afraou unit (plane-polarized light). (**d**) Chloritoid partially replaced by retrograde kaolinite and phengite in the main foliation of the Ras Afraou unit (crossed polars). (**e**) Chlorite–chloritoid–phengite assemblage in the main foliation of the Tres Forcas units. (**f**) Chloritoid–quartz–phengite assemblage in the Khebaba unit (plane-polarized light). Mineral abbreviations after Kretz (1983); and Phg, phengite.

Mineral compositions

Mineral analysis were performed using Cameca SX50 and SX100 electron microprobes (Camparis, University Paris VI) using standard conditions (15 kV, 10 nA) and the following standards: Fe_2O_3 (Fe), $MnTiO_3$ (Mn, Ti), diopside (Mg, Si, Ca), orthoclase (Al, K), albite (Na) and CaF_2 (F). Representative analyses and structural formulae of chlorite, phengite and chloritoid are given in Table 2. Ternary plots for chlorite, chloritoid and phengite compositions are given in Figure 5.

Chloritoid. Chloritoid compositions are very similar in the Ras Afraou, Tres Forcas and Khebaba units. X_{Mg} values vary between 0.05 (Ras Afraou unit) and 0.14 (Tres Forcas unit), with an average value of 0.09, but no significant variations are observed within the different chloritoid populations. The more ferrous compositions are found in the Ras Afraou unit ($X_{Mg} = 0.05$–0.10) and the compositions in the Tres Forcas ($X_{Mg} = 0.08$–0.14) and Khebaba units ($X_{Mg} = 0.06$–0.13) are more Mg-rich.

Chlorite. Chlorite shows very consistent compositions, with an average X_{Mg} value of 0.38 and a Si content in the range 2.5–2.9. As for chloritoid, more Mg-rich compositions are observed in the Tres Forcas ($X_{Mg} = 0.33$–0.48) and Khebaba units ($X_{Mg} = 0.28$–0.45) than in the Ras Afraou unit ($X_{Mg} = 0.34$–0.38).

Phengite. Two phengite populations can be distinguished in the Ras Afraou and Tres Forcas units: phengite from the foliation with a low Si (3.0–3.2) content and a composition close to that of the muscovite end-member, and more substituted phengite (towards the celadonite end-member) with a Si content up to 3.4, which is preserved in quartz segregations (Fig. 5).

First P–T *estimates in the Temsamane units*

The P–T conditions have been derived from stability fields of observed metamorphic assemblages using the PTAX program, a development of the GEO-CALC program (Berman *et al*. 1987). The internally consistent thermodynamic database of Berman (1988) is completed by thermodynamic properties for Mg-carpholite (Vidal *et al*. 1992) and chloritoid (B. E. Patrick & R. G. Berman, unpubl. data). Activity models, based on simple ideal site solution, for Mg-carpholite, chloritoid and chlorite are taken from Vidal *et al*. (1992) and Theye *et al*. (1992), and from Massonne (1995) for phengite. As carpholite has not been found in these units, a theoretical carpholite composition, in equilibrium with chloritoid and chlorite, has been estimated based on partitioning coefficients. Values of $K_D[\mathrm{car/chl}] = (\mathrm{Mg/Fe})_{\mathrm{car}}/(\mathrm{Mg/Fe})_{\mathrm{chl}} = 1.1$ and $K_D[\mathrm{car/cld}] = 6.5$ have been used for carpholite in equilibrium with chlorite and chloritoid, respectively, in agreement with values observed in the Betic Cordilleras or in Crete (Theye *et al*. 1992; Azañón & Goffé 1997). A synthetic grid is presented in Figure 6a, corresponding to the mean compositions observed in the Ras Afraou, Tres Forcas and Khebaba units.

Multi-equilibrium calculations have been performed for the Khebaba unit based on chlorite–chloritoid equilibria (Vidal *et al*. 1999). These estimates were made using the TWQ 2.02 program associated with the Berman (1988) thermodynamic database and completed by thermodynamic data and solid solution models for chlorite (Vidal *et al*. 2001, 2005) and chloritoid (Vidal *et al*. 1994, 1999). Mineral analyses of chlorite were selected following the criteria defined by Vidal *et al*. (2001, 2005) to discard any analysis that cannot be expressed as a linear combination of (Fe,Mg)-amesite, sudoite, clinochlore and daphnite, and the possible Fe^{3+} content in chlorite. Calculations were performed in the FMASH system using chlorite–chloritoid–quartz–water equilibria (Fig. 6b), and the following end-members: clinochlore, daphnite, (Fe,Mg)-amesite and sudoite for chlorites; and (Fe,Mg)-chloritoid. The plotted results (Fig. 6a) correspond to calculation with up to three independent equilibria (Vidal & Parra 2000). Monte Carlo simulation was performed to calculate the error bars on P–T estimates (Fig. 6a) and discard the out-of-equilibrium mineral assemblages (see details given by Vidal & Parra 2000).

In the Ras Afraou, Tres Forcas and Khebaba units, temperature has been estimated based on observed compositions and following the reaction (Fig. 6a)

$$\text{chlorite} + \text{pyrophyllite} = \text{chloritoid} + \text{quartz} + \text{water}.$$

Temperatures have also been estimated using the chlorite–quartz and chlorite–chloritoid thermometers (Vidal *et al*. 1999, 2001).

In the Ras Afraou and Tres Forcas units, pressure has been estimated based on the Si content of phengite ($\mathrm{Si}_{max} = 3.4$) and on the composition of chlorite through the reaction (Fig. 6a)

$$\text{muscovite} + \text{chlorite} + \text{albite} + \text{water} = \text{paragonite} + \text{celadonite}.$$

For the Khebaba units, peak conditions are given by multi-equilibrium calculations based on chlorite–chloritoid–quartz–water equilibria (Fig. 6a and b).

The P–T conditions in the three units are very similar, with pressures around 7–9 kbar for temperatures ranging between 330 and 430 °C (Fig. 6a), and are in agreement with the lack of carpholite in these rocks. Therefore, part of the Temsamane units underwent medium-pressure low-temperature (MP–LT) metamorphism.

Tectonic patterns accompanying metamorphism

To precisely assess the relation between deformation and metamorphism, we complemented the detailed study of Frizon de Lamotte (1985) with some new observations on ductile and brittle structures. Figure 7 synthesizes the structural data collected in the Temsamane units.

Ductile deformation

In the Temsamane units, ductile deformation is characterized by a homogeneous ENE–WSW to NE–SW stretching lineation as described by Frizon de Lamotte (1985) (Fig. 7). In the southern very low-grade metamorphic units, this lineation is marked by clay minerals and rare muscovites or stretched sedimentary clasts and pebbles. Towards the north a more penetrative lineation appears together with increasing metamorphic grade, and is marked by chlorite or micas. The penetrative character of ductile deformation also increases towards the north. In the Ben Tieb and Taferhsit areas (Figs 7 and 8a) deformation is almost coaxial, and characterized by symmetric boudinage structures in the schist or the quartz veins. S–C structures are scarce and the angle between schistosity and the shear planes is low. These structures are also present at a larger scale in the Jurassic marbles of the Taferhsit and Imzirene units. Fold axes are subparallel to the main stretching direction and compatible with a major flattening component in the *yz*-plane of the finite strain ellipsoid (Fig. 7).

In the northern units, sigmoidal quartz veins and S–C shear bands become more frequent (Figs 7 and 8b) and indicate top-to-the-west movements. The Tres Forcas unit, located further to the east, presents similar deformation patterns (Fig. 7). These structures are observed at the microscopic scale and shear bands or sigmoid porphyroblasts are present within the main foliation (Fig. 8c and d). The shear bands are well developed and very penetrative in the Ras Afraou and Tres Forcas units. Deformation is generally more coaxial in the core of the units and becomes more non-coaxial towards tectonic contacts bounding the various units. Intense stretching is observed in the Ras Afraou unit, near Cape Afraou (Fig. 8e and f), with an important flattening component marked by N80–90 folds and boudinage structures (Fig. 8e and g).

In all the units, and particularly in the northern units, small sigmoidal veins, sheared towards the SE, appear in the *yz*-plane. However, these SE-directed structures do not overprint the main foliation and the west-directed structures. Therefore, an additional component of SE shearing seems to be contemporaneous with approximately east–west stretching and a top-to-the-west sense of shear.

Table 2. *Representative electron microprobe analysis of chloritoid, phengite and chlorite in the Temsamane units*

Mineral:	Cld	Cld	Cld	Cld	Cld	Phg	Phg	Phg	Phg	Chl	Chl	Chl	Chl
Sample:	TS0209	TS0326	TF0203	TF0208	TS0305	TS0327	TS0203	TF0208	TF0202	TS0203	TF0208	TS0305	TS0313
Unit:	RA	RA	TF	TF	K	RA	RA	TF	TF	RA	TF	K	K
SiO_2	24.024	23.713	24.275	24.555	23.992	50.098	45.960	50.432	46.985	23.348	24.396	24.028	24.473
TiO_2	0.000	0.020	0.155	0.432	0.139	0.198	0.087	0.000	0.367	0.000	0.033	0.000	0.032
Al_2O_3	40.893	38.786	40.779	41.188	38.258	27.979	34.843	28.712	33.811	22.431	23.268	24.057	24.355
FeO	24.505	28.050	25.432	24.453	27.631	4.147	2.199	3.211	2.242	30.232	28.537	32.322	27.129
MnO	0.940	0.102	0.501	0.479	0.664	0.016	0.009	0.000	0.015	0.328	0.111	0.222	0.272
MgO	1.423	0.859	1.877	2.076	1.466	2.134	0.885	2.283	1.005	9.992	11.253	8.082	11.444
Na_2O	0.070	0.012	0.000	0.032	0.027	0.000	0.000	0.003	0.004	0.000	0.097	0.047	0.014
CaO	0.000	0.000	0.044	0.000	0.000	0.242	0.997	0.221	1.123	0.000	0.253	0.000	0.016
K_2O	0.017	0.015	0.026	0.000	0.000	10.000	9.295	10.058	8.936	0.036	0.066	0.000	0.000
F	0.084	0.259	0.000	0.000	0.033	0.182	0.164	0.179	0.000	0.122	0.067	0.122	0.117
Total	91.956	91.816	93.089	93.215	92.210	95.003	94.472	95.104	94.507	86.500	88.337	88.884	87.853
Structural formula													
Si	2.000	2.008	2.003	2.011	2.030	3.376	3.088	3.376	3.142	2.577	2.605	2.590	2.595
Ti	0.000	0.001	0.010	0.027	0.009	0.010	0.004	0.000	0.018	0.000	0.003	0.000	0.003
Al	4.013	3.871	3.965	3.975	3.815	2.222	2.759	2.265	2.665	2.918	2.928	3.056	3.043
Fe^{2+}	1.706	1.858	1.720	1.649	1.771	0.234	0.124	0.180	0.125	2.791	2.548	2.913	2.405
Mn	0.066	0.007	0.035	0.033	0.048	0.001	0.001	0.000	0.001	0.031	0.010	0.020	0.024
Mg	0.177	0.108	0.231	0.253	0.185	0.214	0.089	0.228	0.100	1.644	1.792	1.299	1.809
Na	0.006	0.001	0.000	0.003	0.002	0.000	0.000	0.000	0.000	0.000	0.011	0.005	0.002
Ca	0.000	0.000	0.007	0.000	0.000	0.032	0.130	0.029	0.146	0.000	0.052	0.000	0.003
K	0.004	0.003	0.005	0.000	0.000	0.860	0.797	0.859	0.762	0.005	0.009	0.000	0.000
F	0.022	0.069	0.000	0.000	0.009	0.039	0.035	0.038	0.000	0.043	0.023	0.042	0.039
Sum	5.994	6.000	6.000	5.965	6.000	6.988	7.030	6.974	6.963	10.011	10.027	9.925	9.922
X_{Mg}	0.091	0.055	0.116	0.131	0.092					0.368	0.412	0.307	0.427

RA, Ras Afraou; TF, Tres Forcas; K, Khebaba.

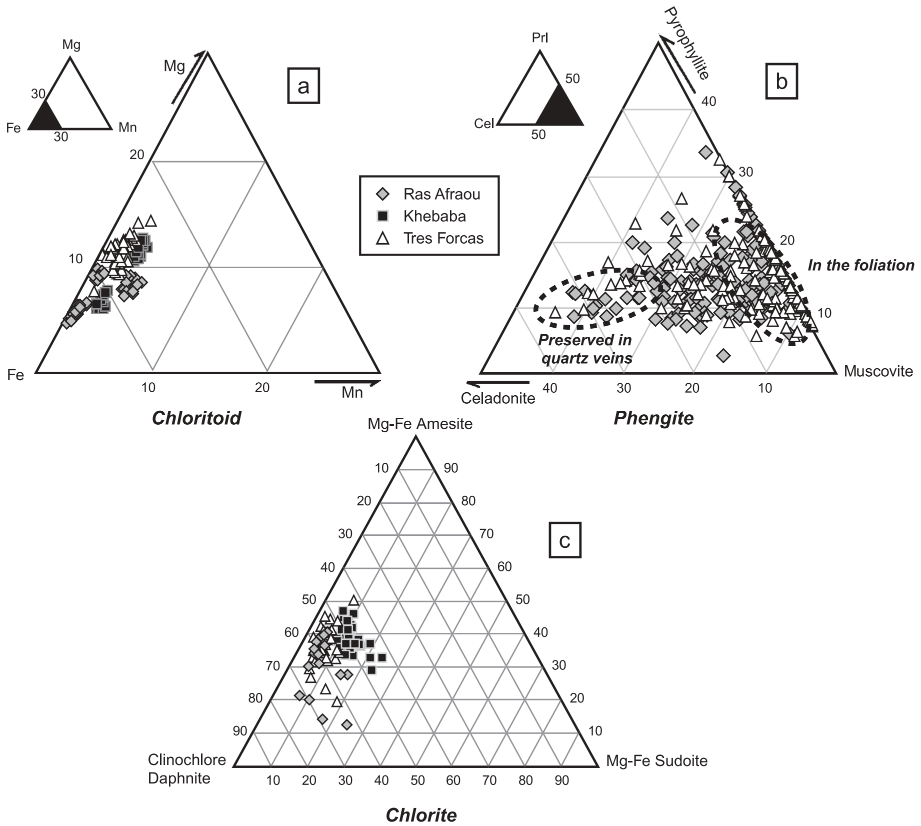

Fig. 5. Mineral compositions for the Ras Afraou, Tres Forcas and Khebaba units. (**a**) Fe–Mn–Mg ternary diagram of chloritoid compositions. (**b**) Celadonite–muscovite–pyrophyllite ternary diagram of phengite compositions. (**c**) Clinochlore–daphnite–(Mg,Fe)amesite–(Mg,Fe)sudoite ternary diagram of chlorite compositions.

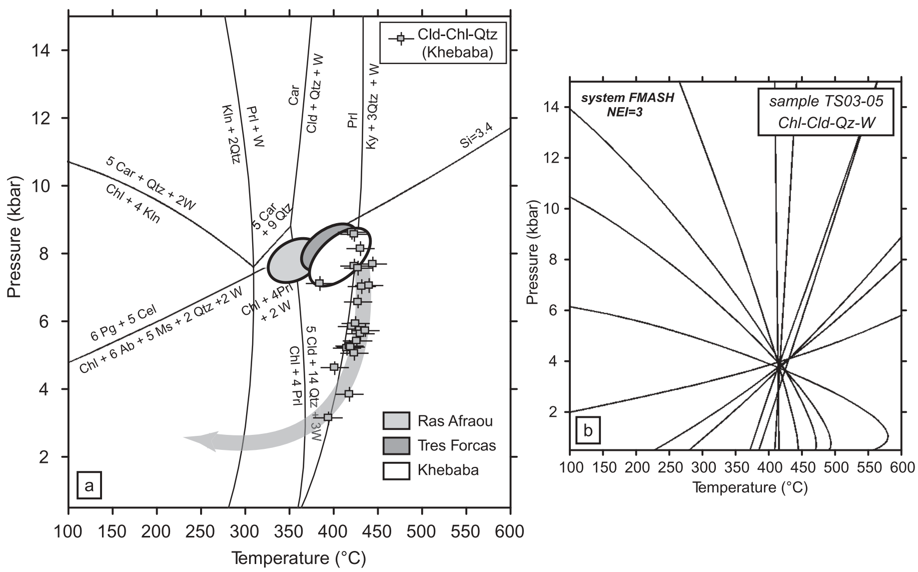

Fig. 6. (**a**) Calculated P–T grid based on observed mineral compositions showing the P–T conditions for the Ras Afraou, Tres Forcas and Khebaba units together with the P–T path calculated for the Khebaba unit. The errors bars are the σP and σT calculated from the Monte Carlo simulation. (**b**) Example of multi-equilibrium calculation for a chlorite–chloritoid–quartz assemblage in the FMASH system. Mineral abbreviations after Kretz (1983); and Car, carpholite; Cel, celadonite; W, water. (See text for details of the calculations.)

The evolution towards brittle deformation

Numerous brittle structures (fibrous veins, tension gashes, fractures), which rework ductile structures, also characterize the Temsamane units (Fig. 7).

The general orientation of these structures is perpendicular to the main ENE–WSW stretching direction observed regionally in all the Temsamane units, including the Tres Forcas outcrop (Fig. 7). Fibrous veins of quartz or calcite crosscut the foliation, and vein poles are generally parallel to the stretching lineation (Figs 7 and 8h). These structures are more numerous near major tectonic contacts. Poles to late fractures also exhibit the same orientation (Fig. 7). Therefore all the ductile and brittle structures indicate the same roughly east–west stretching direction.

Discussion

Reappraisal of the P–T*–deformation history of the Temsamane units*

As a result of recent advances in handling phyllosilicate-rich, high-variant metamorphic assemblages (e.g. Vidal & Parra 2000), our study provides the first quantitative P–T estimates for the Temsamane units, in contrast to the qualitative results of

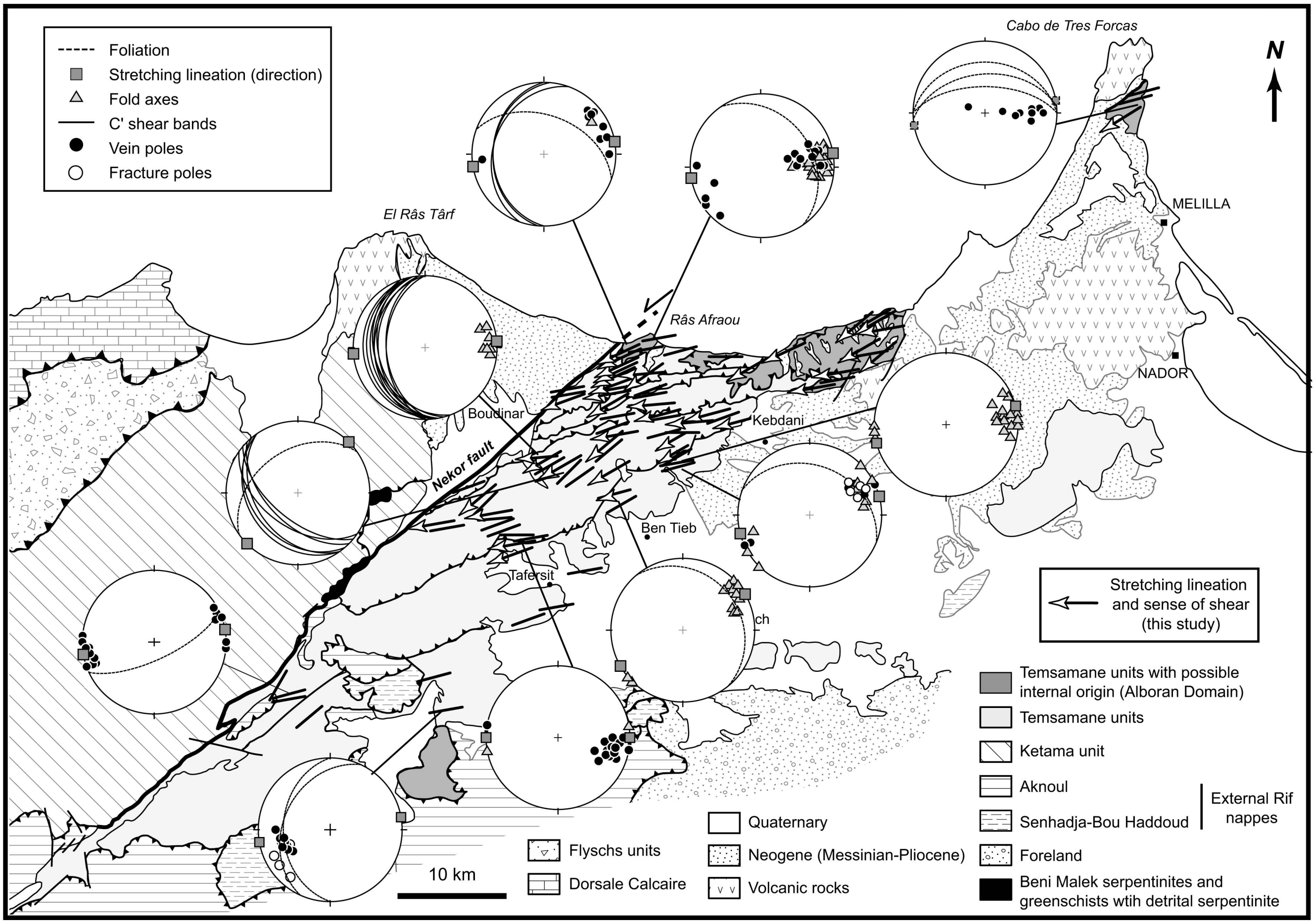

Fig. 7. Tectonic map of the Temsamane units (modified after Frizon de Lamotte 1987) showing the stretching lineations and shear senses together with stereoplots (equal area, lower hemisphere) of ductile and brittle structures (this study).

previous studies (Frizon de Lamotte 1985). Similar *P–T* conditions around 7–9 kbar and 330–430 °C are obtained for the Ras Afraou, Tres Forcas and Khebaba units, which suggests that they could represent remnants of a former single tectonic unit (Fig. 9). These MP–LT conditions differ from those of the other Temsamane units, which were affected only by incipient, low-grade metamorphism.

These three units were thus buried to depths of about 20–25 km along a relatively low burial metamorphic gradient of 13–15 °C km^{-1} typical of subduction zones. Their metamorphism therefore implies the building up of a Rifan accretionary wedge, unlike the development of the other External Rif units. These *P–T* conditions also resemble those of the lower-grade Sebtides of the Alboran Domain (Fig. 9; Bouybaouène *et al*. 1995), which could point to an early common metamorphic history, as discussed below.

The structural observations reported here point to a very coherent tectonic regime throughout the Temsamane units and strengthen earlier conclusions (e.g. Frizon de Lamotte 1985). Ductile deformation, marked by a roughly ENE–WSW stretching direction associated with a top-to-the-west sense of shear, affects the MP–LT units as well as the other Temsamane units. In the Ras Afraou, Tres Forcas and Khebaba units no clear mesoscopic tectonic remnants of the MP–LT metamorphic peak are preserved. At the microscopic scale, chloritoid (together with early, Si-rich phengite) is preserved within pre-S_2 quartz porphyroblasts and as relicts in the main foliation (S_2). In contrast, Phg–Chl ± Kln assemblages are found in the exhumation-related S_2 foliation and shear bands. Also, the orientation of brittle structures shows that the deformation regime associated with roughly east–west stretching and top-to-the-west sense of shear persisted at shallow levels.

Several unpublished preliminary $^{40}Ar–^{39}Ar$ data (Negro 2005) place further constraints on the time frame for the tectonometamorphic evolution of the Temsamane units. The age of the MP–LT metamorphic peak, although not well constrained, could be Oligocene (>23–28 Ma) (Monié *et al*. 1984; Negro 2005), whereas the majority of radiometric constraints associated with east–west stretching and top-to-the-west exhumation are Mid-Miocene (*c*. 15–13 Ma; Negro 2005). The evolution towards late, brittle deformation associated with a prolonged east–west stretching could correspond to the scattered ages obtained in the range 10–8 Ma (Monié *et al*. 1984; Negro 2005). This would be consistent with the occurrence of unconformable Messinian deposits on top of the Temsamane units (Fig. 2b).

Origin of the MP–LT Temsamane units and their place in the External Rif evolution

Internal v. external origin?. The similar lithostratigraphic sequence and subduction-related MP–LT metamorphic conditions

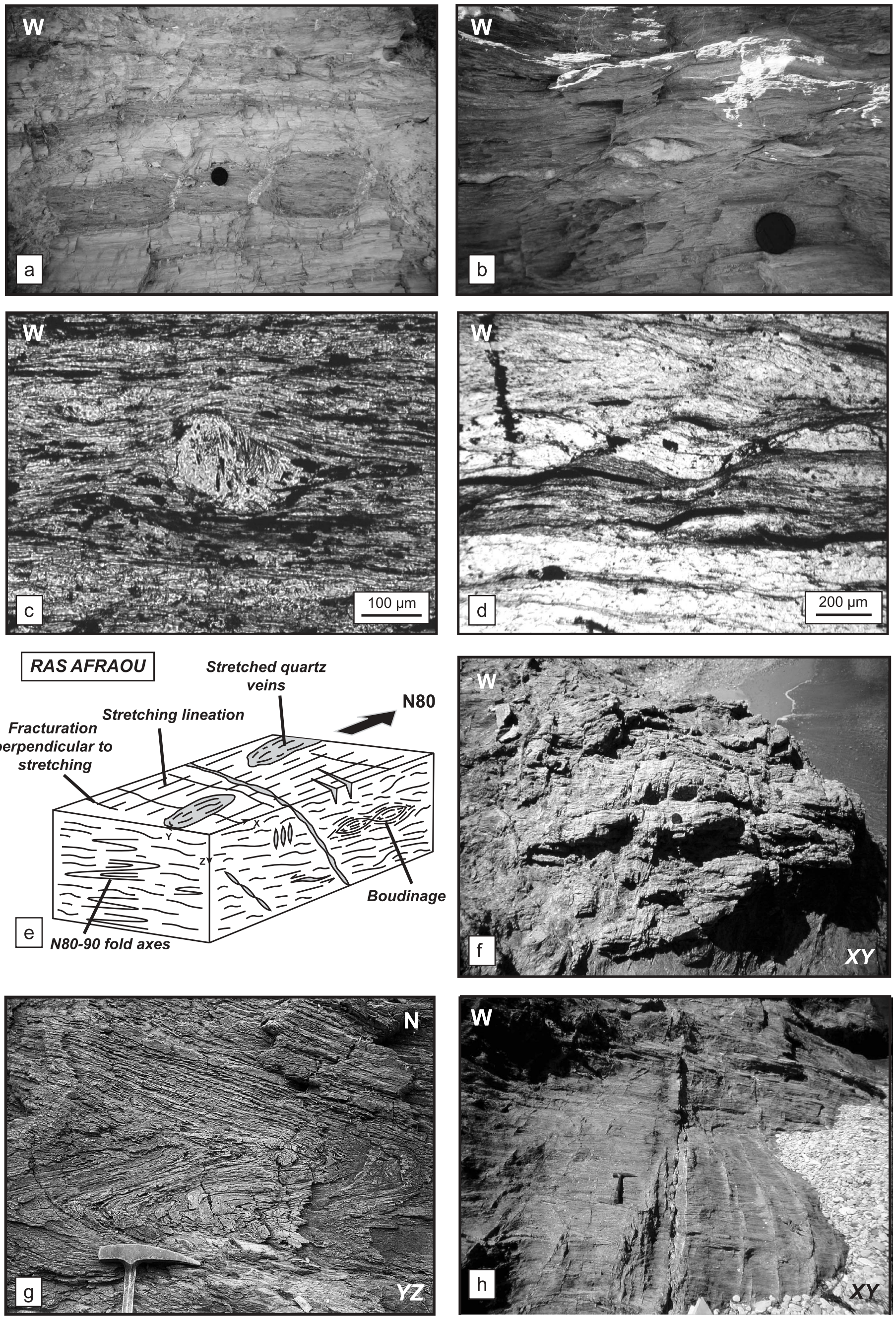

Fig. 8. Photographs and microphotographs of tectonic structures observed in the Temsamane units. (**a**) Boudinage structures, fractures and veins in the Taferhsit unit (II) showing important east–west stretching. (**b**) Sigmoid quartz veins and S–C shear bands in the North Temsamane units. (**c**,**d**) Microphotograph of sheared albite porphyroblast (**c**) and micro S–C shear bands in the main foliation (**d**) indicating top-to-the-west movements. (**e**) Block diagram depicting intense deformation in the Ras Afraou unit. (**f**) Intense deformation of quartz veins underlining the stretching lineation (*xy*-plane). (**g**) N80–90 fold axes affecting the foliation parallel to the main stretching direction (*yz*-plane). (**h**) Late fractures and veins perpendicular to the stretching direction, indicating evolution towards brittle deformation (*xy*-plane).

of the Ras Afraou, Tres Forcas and Khebaba units suggest a possible internal origin for these units. Three alternative tectonic scenarios for the evolution of the External Rif are described below (Fig. 10). The stratigraphic, tectonic and metamorphic arguments supporting these scenarios are listed in Table 3.

Hypothesis 1 (Fig. 10a) assumes that the MP–LT Temsamane units are of internal origin and were subducted together with the Sebtides and later thrust onto the External Rif nappe pile as allochthonous nappes. The major sinistral displacement of the Alboran Domain relative to the African margin during the Miocene (Andrieux *et al*. 1971; Frizon de Lamotte 1985; Leblanc 1990) could have favoured such a juxtaposition of the Alboran Domain units with the Mesorif.

Hypothesis 2 (Fig. 10b) implies the existence of a second, short-lived subduction zone within the Mesorif margin, located further to the south and parallel to the main Sebtides subduction system. Hypothesis 3 (Fig. 10c) suggests that the tectonic positions of the three units result from basement thrusts affecting the Mesorif (Frizon de Lamotte *et al*. 2004). The last hypothesis does not account for the existence of MP–LT metamorphism or for the similarity between Ras Afraou and Khebaba metamorphic imprints. Therefore, we retain Hypotheses 1 and 2 in the discussion below.

Early emplacement of the MP–LT Temsamane units in the External Rif nappe stack. Whatever the correct interpretation regarding the geodynamic scenario (i.e. Hypothesis 1 or 2 described above), the thrusting of the MP–LT Temsamane units necessarily took place after their exhumation at 15–13 Ma and before the emplacement of the Aknoul nappe of supra-Ketama

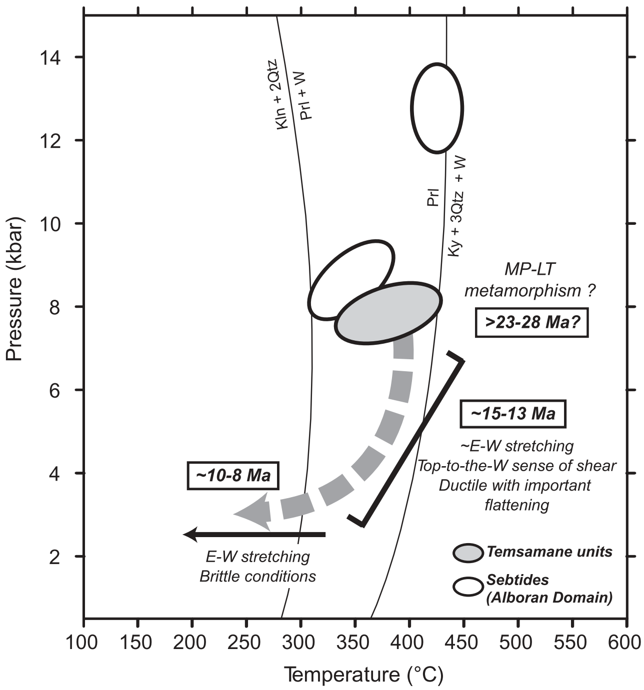

Fig. 9. Synthetic *P–T* grid for the MP–LT Temsamane units with proposed tectonometamorphic evolution and comparison with the Sebtides. Geochronological constraints after Monié *et al*. (1984) and Negro (2005). *P–T* conditions for the Sebtides after Bouybaouène *et al*. (1995) and Vidal *et al*. (1999).

origin (which post-dated the Tortonian; Frizon de Lamotte 1981). The timing of nappe emplacement is shown in Fig. 10a and b, with the successive emplacement of the MP–LT Temsamane, Bou Haddoud–Senhadja and Aknoul nappes. Late thrusts and pop-up structures locally reworked these contacts in the vicinity of Khebaba (Fig. 10a and b; Frizon de Lamotte 1987; Darraz & Leblanc 1989).

A major uncertainty concerns the relationship between the Khebaba and the Ras Afraou–Tres Forcas units: whereas the two latter units are readily linked, the tectonic position of the Khebaba unit is more difficult to assess. Given its structural position and its metamorphic imprint, the Khebaba unit could either belong to the MP–LT Temsamane units proper or represent the metamorphic base of the Senhadja nappe (Figs 10a, b and 11).

A possible tectonic time frame for the Temsamane units. The following tectonometamorphic scenario can be proposed for the Temsamane units.

(1) A first metamorphic stage took place under MP–LT conditions, possibly during the Oligocene or somewhat later, but its age is at present poorly constrained.

(2) The second, major tectonometamorphic event corresponded to the exhumation of the MP–LT Temsamane units during the Middle Miocene (*c*. 15–13 Ma; Negro 2005). This event was accompanied by east–west stretching and top-to-the-west movements along a palaeo-Nekor fault, whose offset was sinistral or normal with respect to the Intrarif. Consistently, apatite fission-track dating for the Ketama units points to ages between 20 and 14 Ma (Azdimousa *et al*. 1998), suggesting that these units were near the surface while the MP–LT Temsamane units were being exhumed.

(3) A third deformation stage associated with continued east–west stretching and brittle–ductile patterns developed as a result of NW–SE compression (*c*. 10–8 Ma; Negro 2005). This event is responsible for the nappe sliding and the emplacement of the MP–LT Temsamane units, together with continued sinistral wrench movements along the Nekor fault (Asebriy *et al*. 1993).

Exhumation of the Temsamane units: a consequence of westward slab retreat during the Middle–Late Miocene?

The Temsamane units in the tectonic and metamorphic evolution of the Rif. Tectonometamorphic and geochronological constraints for the Temsamane units differ from those for both the External Rif and the Alboran Domain. The exhumation of the Temsamane units, associated with roughly east–west stretching and top-to-the-west movements during the Middle Miocene, differs from the exhumation of the Sebtides, characterized by NW–SE to north–south stretching and top-to-the-north shear sense during the Late Oligocene–Early Miocene (Fig. 12a and b). The first post-tectonic sediments overlying the Sebtides are Aquitanian (Feinberg *et al*. 1990), showing that these units were already exhumed in the Early Miocene, whereas they are Messinian in the External Rif. Taking into account palaeomagnetic rotations (Saddiqi *et al*. 1995), the direction of stretching was roughly north–south in the Sebtides during the Late Oligocene–Early Miocene, whereas it was roughly east–west in the Temsamane units during the Middle–Late Miocene. These features suggest a major change in tectonic regime in the Rif during the Early Miocene.

Available geochronological data are too few to determine whether the peak metamorphism was attained coevally or diachronously in the Sebtides and in the Temsamane units, or whether there were only one or two subduction zones (Fig. 10a and b). Data from the at-present ill-constrained chloritoid-bearing metamorphic units of the Tell massif (Algeria; Guardia 1975) should perhaps be the aim of future studies.

Evolution of the Temsamane units in the frame of the Betic–Rif arc. At the regional scale, striking similarities are found to the Nevado–Filábride complex of the Betic Cordilleras (Fig. 12a), which represents the lower part of the Alboran Domain (e.g. Martínez-Martínez *et al*. 2002): (1) the same east–west stretching and top-to-the-west shear sense is found in both the Nevado–Filábride and the Temsamane units; (2) radiometric constraints for the late exhumation stages of the Nevado–Filábride complex also point to Middle to Late Miocene ages (Johnson *et al*. 1997; De Jong 2003; Augier *et al*. 2005), as for the Temsamane units (Monié *et al*. 1984; Negro 2005) and the Ketama unit (Azdimoussa *et al*. 1998; Fig. 12a). The first post-nappe sediments overlying the Nevado–Filábride complex are Tortonian in age (Völk 1967), whereas the Sebtides–Alpujárrides had already been exhumed in the Early Miocene.

As palaeomagnetic studies reveal no significant rotation in the Temsamane area, the observed stretching direction probably reflects the regional-scale direction of extension (e.g. Chalouan & Michard 2004). This regional-scale east–west extension is compatible with the westward slab retreat initiated during the Early Miocene, as proposed by several researchers (Fig. 12c) (e.g. Lonergan & White 1997; Frizon de Lamotte *et al*. 2000; Jolivet *et al*. 2006) and supported by recent tomographic studies (Spakman & Wortel 2004).

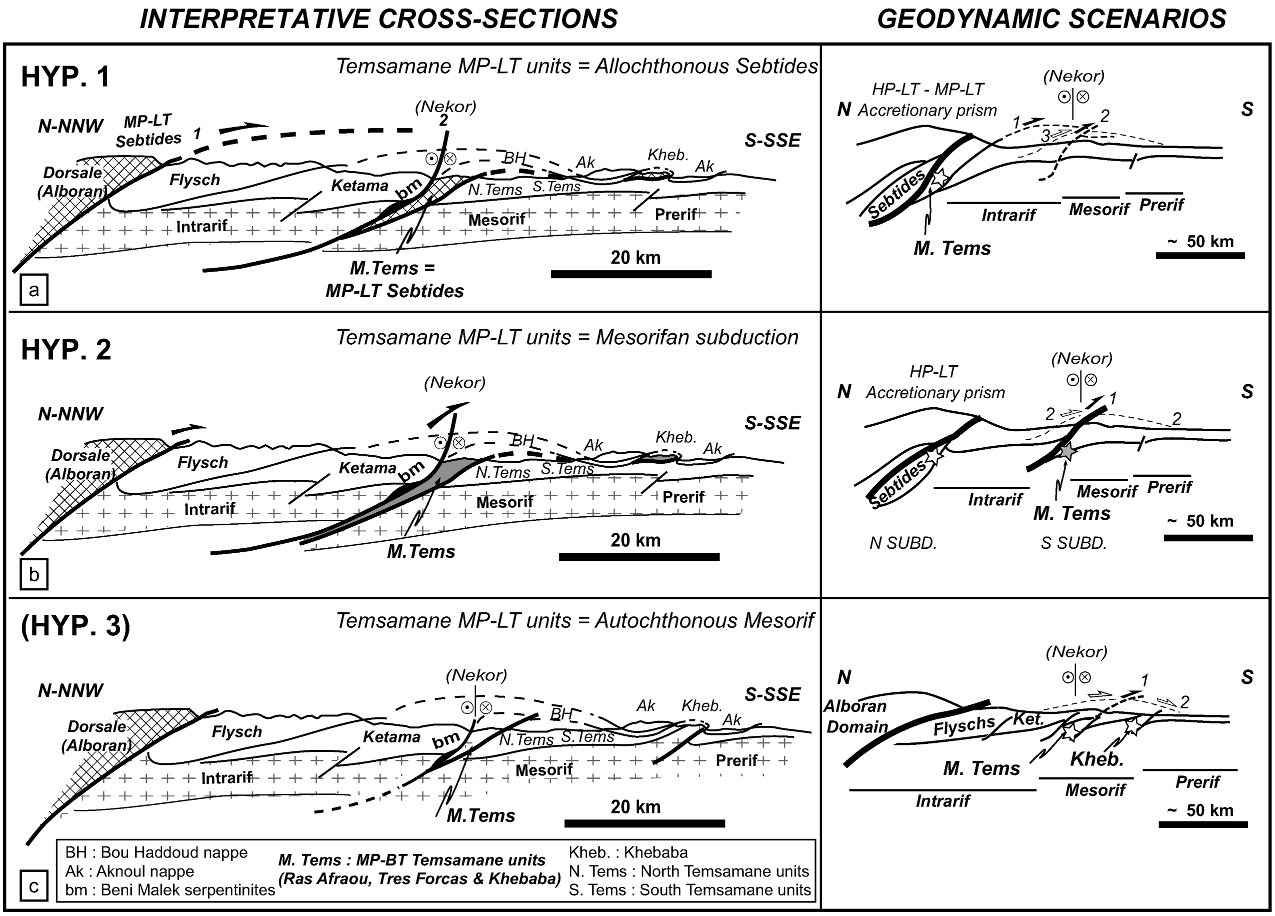

Fig. 10. Alternative scenarios proposed for the origin of the MP–LT Temsamane units with interpretative cross-sections and geodynamic settings. Interpretative cross-section modified after Leblanc (1980), Frizon de Lamotte (1981) and Frizon de Lamotte *et al*. (2004). (See text for details.)

Table 3. *Tectonic, stratigraphic and metamorphic arguments on the origin of the Temsamanes units*

Stratigraphic	Metamorphic	Tectonic
Age of the MP–LT Temsamane protolith: Permo-Trias or Palaeozoic (the only Temsamane unit where Jurassic limestones are lacking) (supports Hypotheses 1, 2 and possibly 3)	Ctd–Phg–Kln parageneses found only in Ras Afraou, Tres Forcas and Khebaba units (supports Hypotheses 1 and 2)	Tectonic position of the Ras Afraou unit on top of the Temsamane units (supports Hypothesis 1)
Similarity of sedimentary facies to Sebtides (supports Hypothesis 1)	Metamorphic conditions of 6–8 kbar and 350–430 °C indicative of a MP–LT subduction zone gradient (supports Hypothesis 1 and possibly Hypothesis 2)	Proximity of the Dorsale towards the west (representing the Sebtides cover) (supports Hypothesis 1)
Gradual decrease of stratigraphic ages across the Temsamane units towards the north (Frizon de Lamotte 1985, p. 41), suggesting a continuity between the MP–LT Temsamane units and the rest (supports Hypotheses 2 and 3)	*P*–*T* conditions similar to those of the lower-grade Sebtides (Alboran Domain) (supports Hypothesis 1)	Continuity of tectonic patterns throughout the Temsamane nappe pile (supports Hypotheses 2 and 3)
	Gradual northward increase of metamorphic grade in the North Temsamane units (supports Hypothesis 2)	Lack of an intra-nappe major tectonic contact (supports Hypotheses 2 and 3)
	Exhumation during the Middle Miocene, whereas Sebtides had already been exhumed (supports Hypotheses 2 and 3)	Presence of post-nappe Messinian sediments (supports Hypotheses 1, 2 and 3)
		Deformed Middle Miocene sediments in the South Temsamane units (supports Hypotheses 2 and 3)

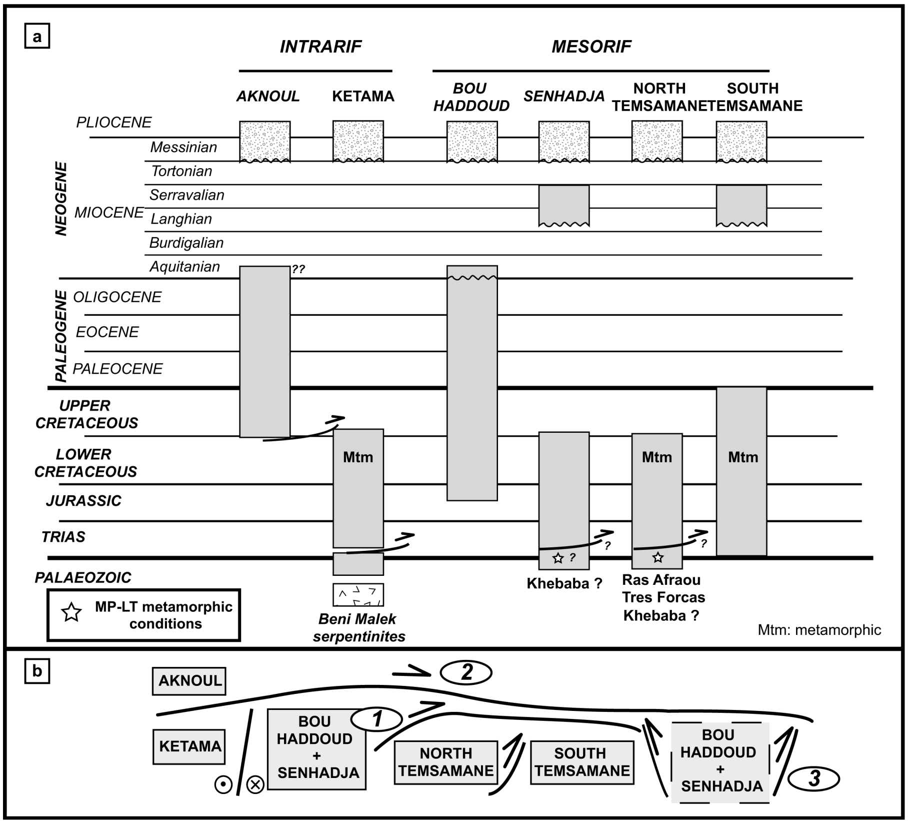

Fig. 11. (**a**) Simplified tectonostratigraphic columns for the Intrarif, the Mesorif and the External Rif nappes showing the position of the metamorphic units, based on Suter (1980) and Frizon de Lamotte (1985). (**b**) Tectonic relationships between the units of the External Rif according to Frizon de Lamotte (1985, 1987). (See text for details.)

Conclusions

This study provides new constraints on the evolution of the External Rif and the geodynamic evolution of the Betic–Rif arc by deciphering the tectonometamorphic evolution of the Temsamane units.

Parts of the Temsamane units recorded MP–LT metamorphic conditions in the range 7–9 kbar and 330–430 °C. These conditions are very similar to those reported for the shallowest HP–LT Alboran Domain units and reflect a rather low burial metamorphic gradient of 13–15 °C km^{-1} typical of subduction zones. These units are characterized by a coherent deformation regime with roughly east–west stretching and top-to-the-west shear sense accompanying the exhumation of the whole Temsamane massif. The age of the metamorphic peak is not well constrained but could be Oligocene (Monié *et al*. 1984; Negro 2005). The main exhumation stage of the Temsamane units occurred during the Middle Miocene (*c*. 15 Ma) and continued under brittle conditions until the Messinian.

To account for this MP–LT metamorphic imprint, two main hypotheses can be put forward: Hypothesis 1 involves an internal origin, with the MP–LT Temsamane units having been subducted together with the Sebtides; Hypothesis 2 involves an external origin, implying the existence of a transient Mesorifan subduction zone, approximately parallel to the main one in the Alboran Domain but located somewhat to the south. At the scale of the entire Rif, however, the late tectonometamorphic evolution of the Temsamane units strongly differs from that of the Sebtide units and resembles the Middle to Late Miocene east–west extension observed in the core of the internal Betics, on the other side of the Alboran Sea. We tentatively relate this late evolution to the onset of westward slab retreat in the Alboran region during the Early Miocene.

The French–Moroccan programme 'Action Intégrée MA/01/13' and the CNRS–INSU are gratefully acknowledged for financial support during field and laboratory work. We warmly thank R. Caron for the quality and the number of thin sections. We are grateful to D. Frizon de Lamotte and G. Booth-Rea for their constructive reviews, and to T. Needham for his constructive comments on the manuscript.

References

Andrieux, J. 1973. Sur le métamorphisme des zones externes du Rif, l'Arc de Gibraltar. *Bulletin de la Société Géologique de France*, **15**(2), 106–107.

Andrieux, J., Fontboté, J.M. & Mattauer, M. 1971. Sur un modèle explicatif de l'Arc de Gibraltar. *Earth and Planetary Science Letters*, **12**, 191–198.

Asebriy, L., Bourgois, J., Cherkaoui, T.E. & Azdimousa, A. 1993. Recent tectonic evolution along the Nekor fault—paleogeographic and structural importance in the External Rif (Morocco). *Journal of African Earth Sciences*, **17**(1), 65–74.

Augier, R., Agard, P., Monié, P., Jolivet, L., Robin, C. & Booth-Rea, G. 2005. Exhumation, doming and slab retreat in the Betic Cordillera (SE Spain): in situ Ar-40/Ar-39 ages and *P–T–d–t* paths for the Nevado–Filábride complex. *Journal of Metamorphic Geology*, **23**(5), 357–381.

Azañón, J.M. & Crespo-Blanc, A. 2000. Exhumation during a continental collision inferred from the tectonometamorphic evolution of the Alpujárride Complex in the central Betics (Alboran Domain, SE Spain). *Tectonics*, **19**(3), 549–565.

Azañón, J.M. & Goffé, B. 1997. Ferro- and magnesiocarpholite assemblages as record of high-*P*, low-*T* metamorphism in the Central Alpujárrides, Betic Cordillera (SE Spain). *European Journal of Mineralogy*, **9**(5), 1035–1051.

Azdimousa, A., Bourgois, J., Poupeau, G. & Montigny, R. 1998. Histoire thermique du massif de Ketama (Maroc); sa place en Afrique du Nord et dans les Cordillères bétiques. *Comptes Rendus de l'Académie des Sciences, Série II*, **326**(12), 847–853.

Balanyá, J.C., García-Dueñas, V., Azañón, J.M. & Sanchez-Gomez, M. 1997. Alternating contractional and extensional events in the Alpujárride Nappes of the Alboran domain (Betics, Gibraltar arc). *Tectonics*, **16**(2), 226–238.

Berman, R.G. 1988. Internally-consistent thermodynamic data for minerals in the

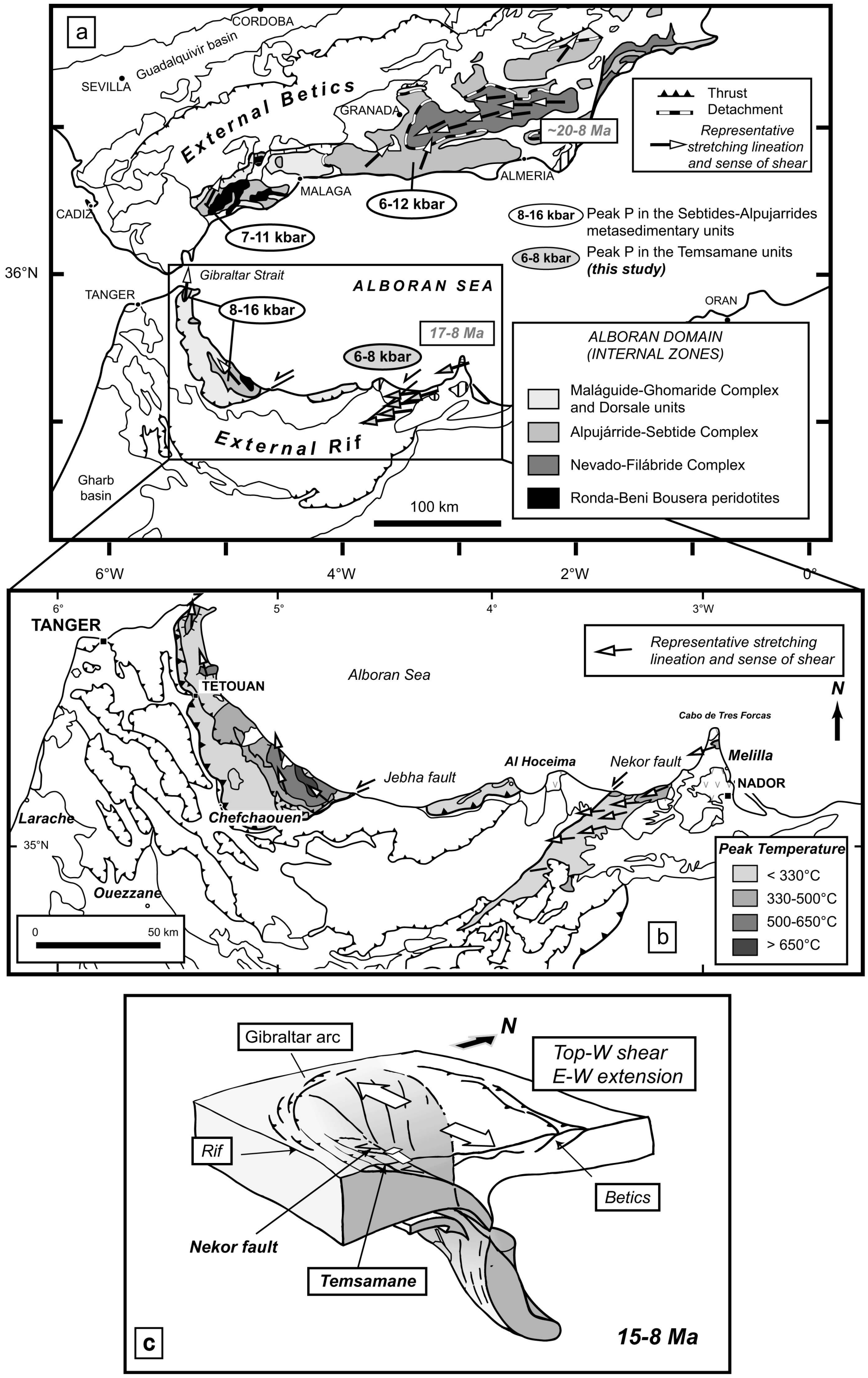

Fig. 12. (**a**) Geological map of the Betic–Rif arc. The peak *P* conditions in the Alboran Domain in the Rif (Bouybaouène *et al*. 1995) and the Betics (Balanyá *et al*. 1997; Azañón & Crespo-Blanc 2000), and the kinematic indicators in the Alboran Domain in the Rif (this study and Saddiqi *et al*. 1988) and the Betics (Balanyá *et al*. 1997; Martínez-Martínez *et al*. 2002) are shown on the map. Geochronological constraints for the exhumation of the Temsamane units (Monié *et al*. 1984; Negro 2005) and the Nevado–Filábride complex (De Jong 2003; Augier *et al*. 2005) are also shown. (**b**) Geological map of the Rif showing peak temperatures (this study and Negro *et al*. 2006) together with kinematic indicators in the Temsamane and Alboran Domain units (this study and Saddiqi *et al*. 1988). (**c**) Block diagram of the Betic–Rif arc geodynamic evolution during the Middle–Late Miocene (modified after Jolivet *et al*. 2006), showing the position and the tectonic evolution of the Temsamane units.

system $Na_2O–K_2O–CaO–MgO–FeO–Fe_2O_3–Al_2O_3–SiO_2–TiO_2–H_2O–CO_2$. *Journal of Petrology*, **29**(2), 445–522.

Berman, R.G., Brown, T.H. & Perkins, E.H. 1987. GEO-CALC—software for calculation and display of *P–T–X* phase-diagrams. *American Mineralogist*, **72**(7-8), 861–862.

Bouybaouène, M.L., Goffé, B. & Michard, A. 1995. High-pressure, low-temperature metamorphism in the Sebtides nappes, northern Rif, Morocco. *Geogaceta*, **17**, 117–119.

Chalouan, A. & Michard, A. 2004. The Alpine Rif belt (Morocco): a case of mountain building in a subduction–subduction–transform fault triple junction. *Pure and Applied Geophysics*, **161**(3), 489–519.

Chalouan, A., Michard, A., Feinberg, H., Montigny, R.A. & Saddiqi, O. 2001. The Rif mountain building (Morocco): a new tectonic scenario. *Bulletin de la Société Géologique de France*, **172**(5), 603–616.

Darraz, C. & Leblanc, D. 1989. Interprétation du massif paléozoïque de Khebaba (Rif oriental, Maroc) comme extrusion d'un lambeau de la nappe externe des Senhadja. *Comptes Rendus de l'Académie des Sciences, Série II*, **308**(1), 71–74.

De Jong, K. 2003. Very fast exhumation of high-pressure metamorphic rocks with excess Ar-40 and inherited Sr-87, Betic Cordilleras, southern Spain. *Lithos*, **70**(3-4), 91–110.

Dewey, J.F., Helman, M.L., Turco, E., Hutton, D.H.W. & Knot, S.D. 1989.

Kinematics of the western Mediterranean. *In:* Coward, M.P., Dietrich, D, & Park, R.G. (eds) *Alpine Tectonics*. Geological Society, London, Special Publications, **45**, 265–283.

Didon, J., Durand-Delga, M. & Kornprobst, J. 1973. Homologies géologiques entre les deux rives du détroit de Gibraltar. *Bulletin de la Société Géologique de France*, **15**(2), 77–105.

Durand-Delga, M., Rossi, P., Olivier, P. & Puglisi, D. 2000. Situation structurale et nature ophiolitique de roches basiques jurassiques associées aux flyschs maghrébins du Rif (Maroc) et de Sicile (Italie). *Comptes Rendus de l'Académie des Sciences, Série II*, **331**(1), 29–38.

Feinberg, H., Maate, A., Bouhdadi, S., Durand-Delga, M., Maate, M., Magne, J. & Olivier, P. 1990. Signification des dépôts de l'Oligocène supérieur–Miocène inférieur du Rif interne (Maroc) dans l'évolution géodynamique de l'arc de Gibraltar. *Comptes Rendus de l'Académie des Sciences, Série II*, **310**(11), 1487–1495.

Frizon de Lamotte, D. 1981. L'olistostrome Tortonien du Nékor et le problème de l'origine du matériel allochtone du Rif externe. *Bulletin de la Société Géologique de France*, **23**(4), 419–426.

Frizon de Lamotte, D. 1985. *La structure du Rif Oriental (Maroc): rôle de la tectonique longitudinale et importance des fluides*. PhD thesis, Université Pierre et Marie Curie, Paris.

Frizon de Lamotte, D. 1987. La structure du Rif externe (Maroc); mise au point sur le rôle des décrochements des chevauchements et des glissements gravitaires. *Journal of African Earth Sciences*, **6**(5), 755–766.

Frizon de Lamotte, D. & Leikine, M. 1985. Métamorphisme miocène du Rif oriental (Maroc) et individualisation de la nappe gravitaire d'Aknoul. *Revue de Géologie Dynamique et de Géographie Physique*, **26**(1), 29–42.

Frizon de Lamotte, D., Saint Bezar, B., Bracene, R. & Mercier, E. 2000. The two main steps of the Atlas building and geodynamics of the western Mediterranean. *Tectonics*, **19**(4), 740–761.

Frizon de Lamotte, D., Crespo-Blanc, A. & Saint-Bézar, B. *et al.* 2004. Transect I: Iberia–Meseta–Guadalquivir Basin–Betic Cordillera–Alboran Sea–Rif–Moroccan Meseta–High Atlas–Sahara Domain. *In:* Cavazza, W., Roure, F.M., Spakman, W., Stampfli, G.M. & Ziegler, P.A.*et al.* (eds) *The TRANSMED Atlas—The Mediterranean Region from Crust to Mantle*. CD-ROM. Springer, Berlin.

Guardia, P. 1975. *Géodynamique de la marge alpine du continent africain d'après l'étude de l'Oranie nord-occidentale*. Thèse de doctorat, Université de Nice.

Hervouet, Y. 1981. Le Massif du Khebaba (Rif Oriental, Maroc): élément de l'unité chaotique de Gareb–Kebdana. *Annales de la Société Géologique du Nord*, **49**(4), 487–490.

Johnson, C., Harbury, N. & Hurford, A.J. 1997. The role of extension in the Miocene denudation of the Nevado–Filábride complex, Betic Cordillera (SE Spain). *Tectonics*, **16**(2), 189–204.

Jolivet, L., Faccenna, C., Goffé, B., Burov, E. & Agard, P. 2003. Subduction tectonics and exhumation of high-pressure metamorphic rocks in the Mediterranean orogens. *American Journal of Science*, **303**, 353–409.

Jolivet, L., Augier, R., Robin, C., Suc, J.P. & Rouchy, J.M. 2006. Lithospheric-scale geodynamic context of the Messinian salinity crisis. *Sedimentary Geology*, **188-189**, 9–33.

Kretz, R. 1983. Symbols for rock forming minerals. *American Mineralogist*, **68**(1-2), 277–279.

Leblanc, D. 1980. L'accident du Nékor et la structure du Rif oriental (Maroc). *Revue de Géologie Dynamique et de Géographie Physique*, **22**(4-5), 267–277.

Leblanc, D. 1990. Tectonic adaptation of the external zones around the curved core of an orogen—the Gibraltar Arc. *Journal of Structural Geology*, **12**(8), 1013–1018.

Lonergan, L. & White, N. 1997. Origin of the Betic–Rif mountain belt. *Tectonics*, **16**(3), 504–522.

Martínez-Martínez, J.M., Soto, J.I. & Balanyá, J.C. 2002. Orthogonal folding of extensional detachments: structure and origin of the Sierra Nevada elongated dome (Betics, SE Spain). *Tectonics*, **21**(3), doi: 10.1029/2001TC001288.

Massonne, H.J. 1995. Experimental and petrogenetic study of UHPM. *In:* Coleman, R.G. & Wang, X. (eds) *High Pressure Metamorphism. Cambridge Topics in Petrology*. Cambridge University Press, Cambridge, 159–181.

Michard, A., Feinberg, H., El-Azzab, D., Bouybaouène, M. & Saddiqi, O. 1992. A serpentinite ridge in a collisional paleomargin setting; the Beni Malek Massif, external Rif, Morocco. *Earth and Planetary Science Letters*, **113**(3), 435–442.

Michard, A., Negro, F., Saddiqi, O., Bouybaouène, M.L., Chalouan, A., Montigny, R. & Goffé, B. 2006. Pressure–temperature–time constraints on the Maghrebide mountain building: evidence from the Rif–Betic transect (Morocco, Spain), Algerian correlations, and geodynamic implications. *Comptes Rendus, Géosciences*, **338**(1-2), 92–114.

Monié, P., Frizon de Lamotte, D. & Leikine, M. 1984. Etude géochronologique préliminaire par la méthode $^{39}Ar/^{40}Ar$ du métamorphisme alpin dans le rif externe (Maroc); précisions sur le calendrier tectonique tertiaire. *Revue de Géologie Dynamique et de Géographie Physique*, **25**(4), 307–317.

Negro, F. 2005. *Exhumation des roches métamorphiques du Domaine d'Alboran: étude de la chaîne rifaine et corrélation avec les Cordillères Bétiques*. Thèse de doctorat, Université Paris XI, Orsay.

Negro, F., Beyssac, O., Goffé, B., Saddiqi, O. & Bouybaouène, M.L. 2006. Thermal structure of the Alboran Domain in the Rif (northern Morocco) and the Western Betics (southern Spain). Constraints from Raman spectroscopy of carbonaceous material. *Journal of Metamorphic Geology*, **24**(4), 309–327.

Saddiqi, O., Reuber, I. & Michard, A. 1988. Sur la tectonique de dénudation du manteau infracontinental dans les Beni Bousera, Rif septentrional, Maroc. *Comptes Rendus de l'Académie des Sciences, Série II*, **307**(6), 657–662.

Saddiqi, O., Feinberg, H., El Azzab, D. & Michard, A. 1995. Paléomagnétisme des péridotites des Beni Bousera (Rif interne, Maroc); conséquences pour l'évolution Miocène de l'Arc de Gibraltar. *Comptes Rendus de l'Académie des Sciences, Série II*, **321**(5), 361–368.

Spakman, W. & Wortel, R. 2004. A tomographic view on Western Mediterranean geodynamics. *In:* Cavazza, W., Roure, F.M., Spakman, W., Stampfli, G.M. & Ziegler, P.A. (eds) *The TRANSMED Atlas—The Mediterranean Region from Crust to Mantle*. Springer, Berlin, 31–52.

Suter, G. 1980. *Carte Géologique de la Chaîne Rifaine. Scale 1/500 000*. Service Géologique du Maroc, Notes et Mémoires, **245a**.

Theye, T., Seidel, E. & Vidal, O. 1992. Carpholite, sudoite and chloritoid in low high-pressure metapelites from Crete and the Peloponnese, Greece. *European Journal of Mineralogy*, **4**, 487–507.

Vidal, O. & Parra, T. 2000. Exhumation paths of high-pressure metapelites obtained from local equilibria for chlorite–phengite assemblages. *Geological Journal*, **35**(3-4), 139–161.

Vidal, O., Goffé, B. & Theye, T. 1992. Experimental study of the stability of sudoite and magnesioferro- and magnesiocarpholite and calculation of a new petrogenic grid for the system $FeO-MgO-Al_2O_3-SiO_2-H_2O$. *Journal of Metamorphic Geology*, **10**, 603–614.

Vidal, O., Theye, T. & Chopin, C. 1994. Experimental study of chloritoid stability at high-pressure and various fO(2) conditions. *Contributions to Mineralogy and Petrology*, **118**(3), 256–270.

Vidal, O., Goffé, B., Bousquet, R. & Parra, T. 1999. Calibration and testing of an empirical chloritoid–chlorite Mg–Fe exchange thermometer and thermodynamic data for daphnite. *Journal of Metamorphic Geology*, **17**(1), 25–39.

Vidal, O., Parra, T. & Trotet, F. 2001. A thermodynamic model for Fe–Mg aluminous chlorite using data from phase equilibrium experiments and natural pelitic assemblages in the 100 degrees to 600 degrees C, 1 to 25 kb range. *American Journal of Science*, **301**(6), 557–592.

Vidal, O., Parra, T. & Vieillard, P. 2005. Thermodynamic properties of the Tschermak solid solution in Fe-chlorite: application to natural examples and possible role of oxidation. *American Mineralogist*, **90**(2-3), 347–358.

Völk, H.R. 1967. Relations between Neogene sedimentation and late orogenic movements in the Eastern Betic Cordilleras (SE Spain). *Geologie en Mijnbouw*, **46**, 471–474.

Wildi, W. 1983. La chaîne tello-rifaine (Algerie, Maroc, Tunisie); structure stratigraphie et évolution du Trias au Miocène. *Revue de Géologie Dynamique et de Géographie Physique*, **24**(3), 201–297.